Egypt. J. Rad. Sci. Applic. **Vol. 38,** No.1-2, pp. 1-11 (2025)

Egyptian Journal of Radiation Sciences and Applications
http://ejrsa.journals.ekb.eg/

Ivermectin Mitigates Lung Toxicity Induced by γ-radiation in Rats *via* TLR4/ NF-κB /MAPK Pathways

Shereen M. El kiki*, Shereen M. Galal, Eman M. El Gazzar, Heba H. Mansour
Health Radiation Research Department, National Center for Radiation Research and Technology, Egyptian Atomic Energy Authority, Cairo, Egypt

RADIATION is capable of inducing reactive oxygen species (ROS), cytokines, chemokines, and growth factors as well as inflammatory cells. Radiation has been termed pro-inflammatory in nature. The current study aims to assess the protective effects of ivermectin against high doses of γ-irradiation by inspecting the effect on inflammatory mediators such as lung receptors toll-like receptors (TLR4), transforming growth factor beta (TGF-β), fibroblast growth factor (FGF), and nuclear factor-kappa B (NF-κB) in adult male albino rats. Ivermectin was administered orally for 14 days at a dose of 3.7 mg/kg/day and then male albino rats were subjected to a high dose of γ-radiation (30 Gy), which was divided into 10 fractions five times per week. In addition to increasing the activity of lactate dehydrogenase A (LDHA) in lung tissue, gamma radiation also significantly disrupted the antioxidant system, resulting in lung damage through increased levels of prostaglandin 2 (PGE2), TLR4, TGF-β, NF-κB, and FGF. In the present work, ivermectin minimized pulmonary damage, through suppression of ROS formation and the restoration of virtually normal levels of FGF, PGE2, TGF-β, NF-κB, and TLR4 in the lungs, as well as the activities of MAPK and LDHA. The biochemical outcomes were validated by the histological analysis. In conclusion, Ivermectin protects against γ-radiation-induced lung damage by lowering fibroblast differentiation, production of reactive oxygen species and cytokines. Ivermectin mitigates lung damage by modulating TLR4/NF-κB /MAPK pathways.

Keywords: Ivermectin; γ-radiation; TLR4; MAPK; NF-κB

Introduction

Destruction of the surrounding healthy tissues delays the ionizing radiation (IR), that is used to treat cancer and causes severe side effects. Pneumonitis and pulmonary fibrosis are the most frequent significant side effects of radiation therapy in patients with breast or thoracic cancer. These conditions might hinder the effectiveness of therapeutic radiation doses and have negative consequences on cancer patients (Rengachar et al., 2022; Wan et al., 2022). The process of radiation-induced lung damage is complex and leads to the production of collagen, the infiltration of inflammatory cells, and the eventual development of fibrosis. This is achieved through the accumulation, proliferation, and differentiation of fibroblasts and myofibroblasts, which in turn causes the excessive generation of reactive oxygen species (ROS), cytokines, growth factors, and extracellular matrix (ECM) deposition (Rengachar et al., 2022; Jin et al., 2020). Thus, the main way to prevent fibrosis is to limit the development of myofibroblasts caused by radiation (Jin et al., 2020).

Besides directly causing a double-strand break in DNA, ionizing radiation also hydrolyzes water and other molecules, producing ROS. These combine with DNA and other cellular components to cause cell deficiency and apoptosis. Moreover, ROS may even activate a strong immune response prior to tissue damage being induced (Jin et al., 2020; Bledsoe et al., 2017). In addition, cytokine

*Corresponding author: E-mail: shereenelkiki@yahoo.com
Received 17/10 / 2024 ; Accepted 16 / 1 / 2025
DOI: 10.21608/EJRSA.2025.326414.1175

cascades that stimulate inflammation can also produce ROS (Wan et al., 2022). Activated inflammatory cells participate in the inflammation process; these cells emit increased levels of inflammatory chemicals, including prostaglandin 2 (PGE2), nitric oxide (NO), tumor necrosis factor alpha (TNF-α), and transforming growth factor beta (TGF-β1). (Azab et al., 2017; Wei et al., 2019).

Toll-like receptors (TLRs) exist on the cell surfaces of immunological, vascular, smooth muscle, and inflammatory cells (Mitsui et al., 2020). Ionizing radiation produces ROS, which in turn activates TLR4 in conjunction with nuclear factor-kappa B (NF-κB) release and increased cytokine generation, such as TNF-α. These events then start a series of events that include the ROS/RNS pathways and mitogen-activated protein kinase p38 (MAPK) cascade (Lotfy et al., 2022). MAPK signaling pathways are known to regulate TLR4 expression based on the differentiation state of the cell (Yoshino et al., 2014). Thus, radiation-induced lung damage may be treated and prevented via the NF-κB / c-Jun N-terminal kinase (JNK) / MAPK pathway (Wan et al., 2022).

Ivermectin is an antiparastic medication licensed by the Food and Drug Administration (FDA) for the treatment of helminthiases, scabies, and onchocerciasis (Yang et al., 2020). Using a 16-membered macrocyclic lactone structure, ivermectin is a macrolide antiparasitic medication used to treat parasitic infestations and prevent viral replication (Foy et al., 2019). By interfering with numerous essential structural and nonstructural proteins, ivermectin stops the virus from reproducing in vitro (Gupta et al., 2022). Recent studies conducted in vitro have also revealed that ivermectin has a promising inhibitory effect on SARS-CoV-2 replication in the earliest stages of infection (Caly et al., 2020; Zaidi & Dehgani-Mobaraki, 2022). Ivermectin's in vitro anti-SARS-CoV-2 activity is assumed to be most likely targeted at the RNA-dependent RNA polymerase (RdRp)-ivermectin complex. As a result, coronavirus transcription and replication are inhibited within the host cell (Swargiary, 2020).

According to Yan et al. (2011), ivermectin considerably reduces the generation of cytokines and the recruitment of immune cells in the mouse bronchoalveolar lavage fluids, demonstrating positive therapeutic benefits in the treatment of asthma.Numerous studies have demonstrated the antinflammatory properties of ivermectin through its inhibition of cytokine production after exposure to lipopolysaccharide (LPS), downregulation of NFκB transcription, and limitation of the formation of both NO and PGE2. (Zhang et al., 2008; Kory et al, 2021).

The study was directed to investigate the hypothesis that Ivermectin may protects against the lung toxicity induced by γ-radiation. Histological and biochemical examinations were used to explore the impact of Ivermectin on lung toxicity.

Materials and Methods

Drug

The supplier of ivermectin (Iversine®) was Universal Pharmaceutical Industries Co. (Unipharma), located in Cairo, Egypt. Drug has been instantly dissolved in physiological saline to provide the desired dosage. All additional chemicals and solvents utilized were of the highest purity grade accessible.

Irradiation

An AECL 137Cs Gamma Cell-40 biological irradiator performed gamma radiation at The National Centre for Radiation Research and Technology (NCRRT), Egyptian Atomic Energy Authority, Cairo, Egypt. At a dose rate of 0.012 Gy/s, a total dose of 30 Gy fractionated into 10 fractions, 5 fractions per week. It had been demonstrated that this radiation dose led to pulmonary toxicity in rats (El kiki *et al.,* 2021).

Experimental animals

Twenty adult male (6 weeks old) *Wistar rats* weighing between 120 and 150 g were taken from the NCRRT's breeding facility. The animals were acclimatized for 7 days and during this period they maintained a commercial standard pellet diet and water *ad libitum*. Animals were kept under natural light/dark cycle conditions, 25 ± 2 °C.

The National Center for Radiation Research and Technology's Ethics Committee conducted all animal procedures in compliance with the US National Institutes of Health's "Guide for the Care and Use of Laboratory Animals" (NIH publication, No. 21A/22, 1996).

Experimental design

Prior to the test, the animals were acclimated to the laboratory environment. The rats were separated into four groups after a seven-day period of adaption (5 rats/group).

Control group: for 14 days, rats received an oral 0.5 ml saline dosage every day. Irradiation Group (IR): rats received 0.5 ml of saline orally every day for 14 days. They were also given a total dosage of 30 Gy in 10 fractions, 5 fractions each week, of radiation. Ivermectin group: rats were administered Ivermectin (3.7 mg/kg body weight, orally) dissolved in saline for 14 consecutive days. The dosage is the same as the 36 mg/day of ivermectin prescribed for humans in the Egyptian protocol for the treatment of mild to moderate cases of COVID-19. (Elfakharany et al., 2021).

Ivermectin + IR group: Rats received a daily oral dose of 3.7 mg/kg body weight of ivermectin for 14 days prior to 30 Gy of fractionated radiation, exposed five times a week.

Collection of tissue samples for analysis

Animals were anesthetized with ketamine (40 mg/kg)/xylazine (4 mg/kg) i.p., then were sacrificed by decapitation, 24 hours after the final dosage of the specified therapy, and lungs were quickly excised. Using a Branson sonifier (250, VWR Scientific, Danbury, Conn., USA), a portion of the lung was cleaned with saline solution, wiped on filter paper, and then homogenized in saline solution. The homogenates were centrifuged at 800 g for 5 min at 4 ºC and the resulting supernatant was centrifuged (Eppendorf AG, centrifuge 5804R, Hamburg, Germany) at 15000 g for 30 min at 4 ºC to get the post-mitochondrial supernatant for measuring superoxide dismutase (SOD).

The homogenates were utilized to assess the levels of (FGF), (TGFβ1), Nitric oxide (NO), malondialdehyde (MDA), (PGE2), (NF-κβ), (TLR4), and reduced glutathione (GSH) content. Also, the activities of mitogen-activated protein kinase (MAPK), (LDHA), and (SOD) were measured. A distinct piece of lung from multiple groups was employed for the histopathological analysis.

Estimation of oxidative stress biomarkers

Using the method described by Minami and Yoshikawa (1979), SOD activity was assessed. Methods of Ignarro et al. (1987) and Ellman (1959) were used to determine the total NO level and GSH content in lung tissues, respectively. Using a colorimetric procedure based on Buege and Aust's methodology, MDA levels were assessed as a sign of lipid peroxidation (Buege & Aust 1978).

Determination of TGF-β1, FGF, and PGE2 by ELISA

The enzyme-linked immunosorbent assay (ELISA) kits from Cloud-Clone Corp., USA; My BioSource, USA; Cusabio, USA; and E-labscience Biotechnology Inc., USA were used to estimate TGF-β1, FGF, PGE2, and LDHA, respectively. The kits were read using an ELISA microplate reader (DV 990 BV 4/6; Gio. De Vita & Co., Rome, Italy) in accordance with the manufacturer's instructions.

Determination of MAPK activity, NF-κβ, and TLR4 by western blot

The Ready-Prep TM protein extraction kit (total protein) provided by Bio-Rad Inc (Catalog #163-2086) was employed according to manufacturer instructions and was added to each sample of the homogenized tissues of all different groups. Bradford Protein Assay Kit (SK3041) for quantitative protein analysis was provided by Bio Basic Inc (Markham Ontario L3R 8T4 Canada). A Bradford assay was performed to determine protein concentration in each sample. 20 µg protein concentration of each sample was then loaded with an equal volume of 2x Laemmli sample buffer containing 4% sodium dodecyl sulfate (SDS), 10% 2-mercaptoethanol, 20% glycerol, 0.004% bromophenol blue and 0.125 M Tris HCl. The pH was brought to 6.8. Each previous mixture was boiled at 95°C for 5 minutes to ensure protein denaturation before loading on polyacrylamide gel electrophoresis. Polyacrylamide gels were performed using TGX Stain-Free™ FastCast™ Acrylamide Kit SDS-polyacrylamide gel electrophoresis (SDS-PAGE) was provided by Bio-Rad Laboratories Inc Cat # 161-0181. The SDS-PAGE TGX Stain-Free Fast Cast was prepared according to manufacturer instructions. The gel was assembled in a transfer sandwich placed in the transfer tank with 1x transfer buffer, composed of 25 mM Tris and 190 mM glycine, and 20% methanol. Then, the blot was run for 7 min at 25 V to allow protein bands to transfer from the gel to the membrane using BioRad Trans-Blot Turbo. The membrane was blocked in tris-buffered saline with Tween 20 (TBST) buffer and 3% bovine serum albumin (BSA) at room temperature for 1 hr. In TBST, primary antibodies of MAPK, NF-κβ, and TLR4 were diluted following the manufacturer's recommendations. Incubation was done overnight in each primary antibody solution, against the blotted target protein, at 4°C. For 5 minutes the blot was rinsed with

TBST 3-5 times. For 1 hr at room temperature, the blotted target protein was incubated in the HRP-conjugated secondary antibody (Goat anti-rabbit IgG- HRP-1mg Goat mab-Novus Biologicals) solution, then rinsed with TBST 3-5 times. The chemiluminescent substrate (Clarity TM Western ECL substrate Bio-Rad cat #170-5060) was applied to the blot as directed by the manufacturer. Briefly, equal quantities from solution A (Clarity western luminal/enhancer solution) and solution B (peroxidase solution) were added. To record the chemiluminescent signals A CCD camera-based imager was used. Image analysis software was used to compare the band intensity of the target proteins to the control sample -actin (housekeeping protein) using protein normalization on the ChemiDoc MP imager (Salami and Karami-Tehrani, 2003).

β-actin antibody was acquired from Biolegend, USA, and Rabbit Anti-MAPK Monoclonal Antibody was purchased from Creative Biolabs, USA. NFκB p65 a mouse monoclonal antibody and rabbit polyclonal antibody of TLR4 were bought from Santa Cruz Biotechnology, INC.

Histopathological examination

A distinct section of the lung tissue specimen was taken from each animal group and stored in 10% neutral buffered formalin. Following the procedures outlined by Bancroft et al. (2013), the fixed specimens were split into smaller pieces, washed, and dehydrated in increasingly stronger alcohol. They were then cleared in xylene, imbedded in paraffin, sectioned at 4-6 μm thickness, and stained with hematoxylin and eosin. Prepared slide sections were stained with hematoxylin and eosin, and the results were examined under a light digital microscope (Olympus xc30, Tokyo, Japan). A score ranging from 0 to 4 was assigned to each lung tissue section according to the extent of interstitial inflammation, thickening of the alveolar wall, inflammation in the peribronchi, and interstitial edema (0 ≤ 10%, 1 = up to 30%, 2 = up to 50%, 3 = up to 70%, 4 ≥ 70%) (Eldh et al., 2012).

Statistical data analysis

One-way analysis of variance (ANOVA) and Tukey's multiple comparison tests were used in the statistical analysis of all the data using the program Prism 5.0 (Graph Pad, San Diego, CA, USA). The significances were be considered at $P < 0.05$. The data is shown as means ± SEM.

Results

Biochemical results

TGF-β1, FGF, PGE2 levels and LDHA activity:

When compared to the control, radiation exposure significantly raised the levels of pulmonary TGF-β1, FGF, and PGE2 (260.1%, $P < 0.05$, 269.6%, $P< 0.05$& 240.9%, $P< 0.05$, respectively), but ivermectin therapy attenuated the increases in these markers of lung injury caused by radiation (57.2% decrease, $P < 0.05$, 52.85 % decrease, $P< 0.05$ & 47.86 % decrease, $P< 0.05$, respectively) compared to radiation group (Fig. 1 A, B, and C). Furthermore, when compared to the control, radiation exposure dramatically raises lung LDHA activity (354.7% increase, $P < 0.05$). The administration of ivermectin with irradiation reduced pulmonary LDHA activity (45.64% decrease, $P< 0.05$) when compared to the irradiated rats (Fig. 1D).

Oxidative stress

The activity of pulmonary SOD was considerably downregulated (65.6% decrease, $P < 0.05$) in rats subjected to a fractionated dose of gamma radiation (30 Gy in 10 fractions, 5 fractions per week) as compared to the control group (Fig. 2A). While the administration of ivermectin in concomitant with radiation considerably reduced this decrease (71.2% increase, $P < 0.05$). Furthermore, ivermectin treatment prevented the considerable drop in lung GSH (60.9% decrease, $P < 0.05$) that resulted from exposure to gamma radiation (Fig. 2B). In rats exposed to radiation, there was a significant increase in pulmonary MDA and NO levels (173.2% increase, $P < 0.05$ & 187.3% increase, $P < 0.05$); however, the treatment of ivermectin reduced the increase in these levels caused by radiation (37.7% decrease, $P < 0.05$ & 33.5% decrease, $P < 0.05$) (Fig. 2 C and D).

MAPK, TLR4, and NF-κB proteins expression

In comparison to the control group, radiation exposure increased the proteins expression of MAPK, TLR4, and NF-κβ in the pulmonary tissues (223% increase, $P < 0.05$, 293.4% increase, $P < 0.05$ & 291% increase, $P < 0.05$). Compared to the irradiated animals, the ivermectin therapy in concomitant with radiation reduced the protein expression of MAPK, TLR4, and NF-κB (59.1% decrease, $P < 0.05$, 55.8% decrease, $P < 0.05$ & 57.03% decrease, $P < 0.05$) (Fig. 3).

Histopathological results

The lungs of the control and ivermectin groups had normal lung architecture, fine, delicate inter-alveolar septa separating the airspaces and normal vasculature with little perivascular connective tissue, folded columnar epithelial cells of bronchiole, and normal fibrous tissues distribution. The alveoli appeared inflated with thin inter-alveolar septa score of 0 (Fig. 4 a-b).

The interstitium of animals treated to a cumulative dosage of 30 Gy gamma radiation (10 fractions, 5 fractions/week) was shown to be infiltrated by mononuclear cells, primarily lymphocytes and macrophages, in the peribronchial and perivascular regions. Numerous focal emphysematous areas were accompanied by giant alveoli formation that formed enormous alveoli. Marked thickening of the inter-alveolar septa and metaplasia of bronchiolar epithelial lining to stratified squamous cells with complete loss of goblet cells were detected score 3 (Fig. 4c). On the other hand, in comparison to the prior group, the animals exposed to radiation and given ivermectin exhibited a noticeable improvement. Mild thickening of alveolar interstitium was noticed in score 1 (Fig. 4d)

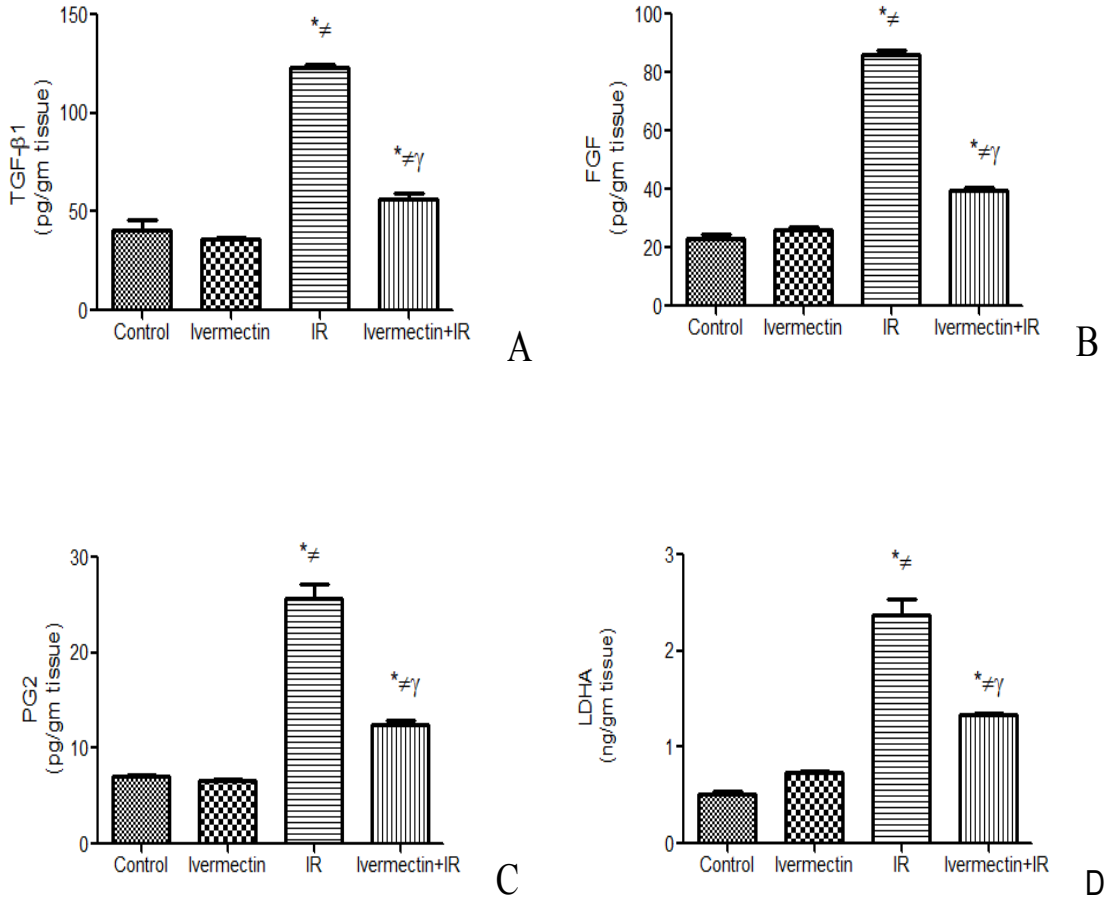

Fig.1. Impact of ivermectin, irradiation (IR), and their combination on (A) transforming growth factor β (TGF-β1) level, (B) fibroblast growth factor (FGF) level, (C) prostaglandin (PGE2) level and (D) lactate dehydrogenase A (LDHA) activity in rat pulmonary tissue. The data is shown as mean ± SE (five rats per group). Using ANOVA and Tukey-Kramer as a post-ANOVA test, *, ≠, and γ indicate substantially different from the control group, ivermectin group, and irradiated group, respectively, at $p \leq 0.05$.

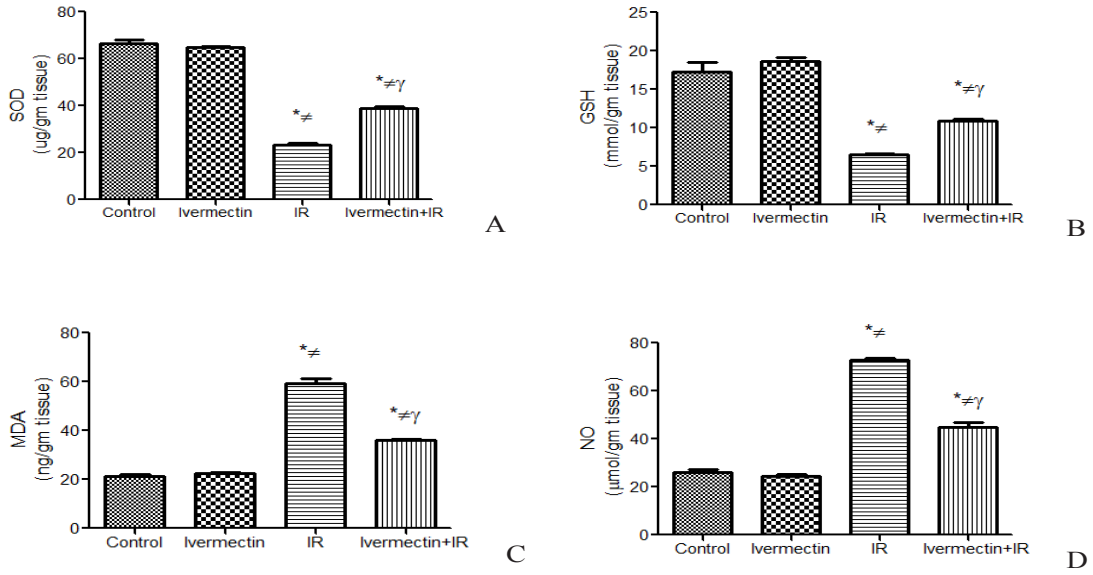

Fig. 2 . Impact of ivermectin, irradiation (IR), and their combination on (A) superoxide dismutase activity (SOD) level (B) glutathione content (GSH) level, (C) malondialdehyde (MDA) level and (D) nitric oxide (NO) level in rat pulmonary tissue. The data is shown as mean ± SE (five rats per group). Using ANOVA and Tukey-Kramer as a post-ANOVA test, *, ≠, and γ indicate substantially different from the control group, ivermectin group, and irradiated group, respectively, at $p \leq 0.05$.

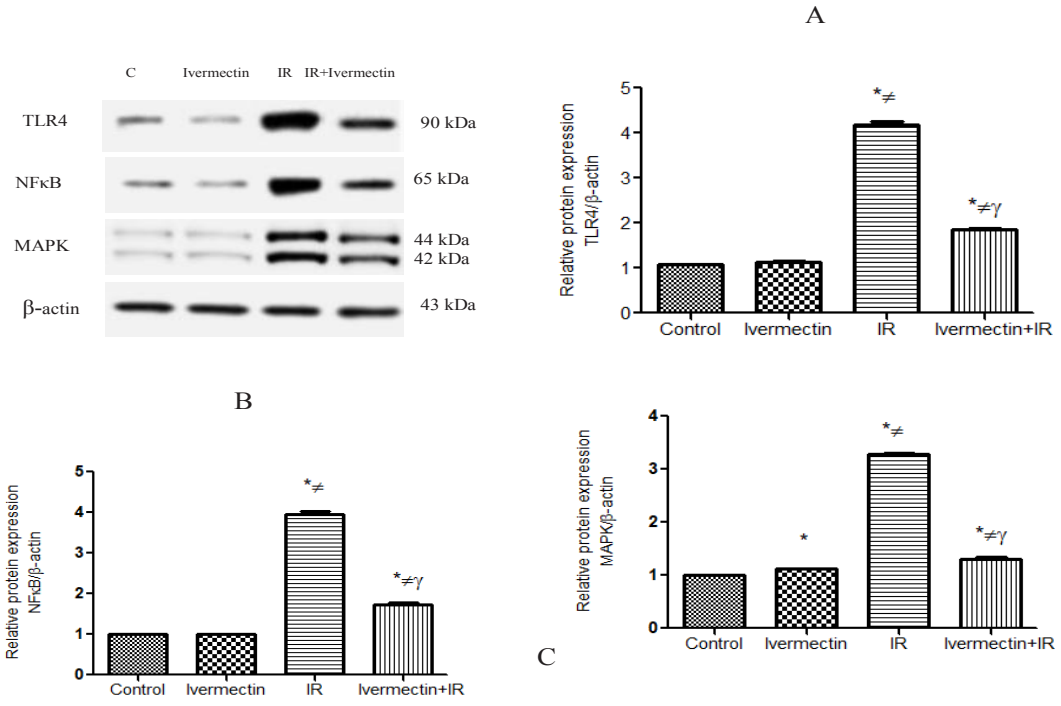

Fig. 3. Impact of ivermectin, irradiation (IR), and their combination on (A) Toll-like receptors (TLR4) (B) Nuclear factor kappa B (NF-κB), (C) Mitogen-activated protein kinase (MAPK), protein expression in rat pulmonary tissues. The β-actin was used to ensure equal protein loading. Relative protein expression was quantified by densitometry and corrected by reference to -actin. The data is shown as mean ± SE (five rats per group). Using ANOVA and Tukey-Kramer as a post-ANOVA test, *, ≠, and γ indicate substantially different from the control group, ivermectin group, and irradiated group, respectively, at $p \leq 0.05$.

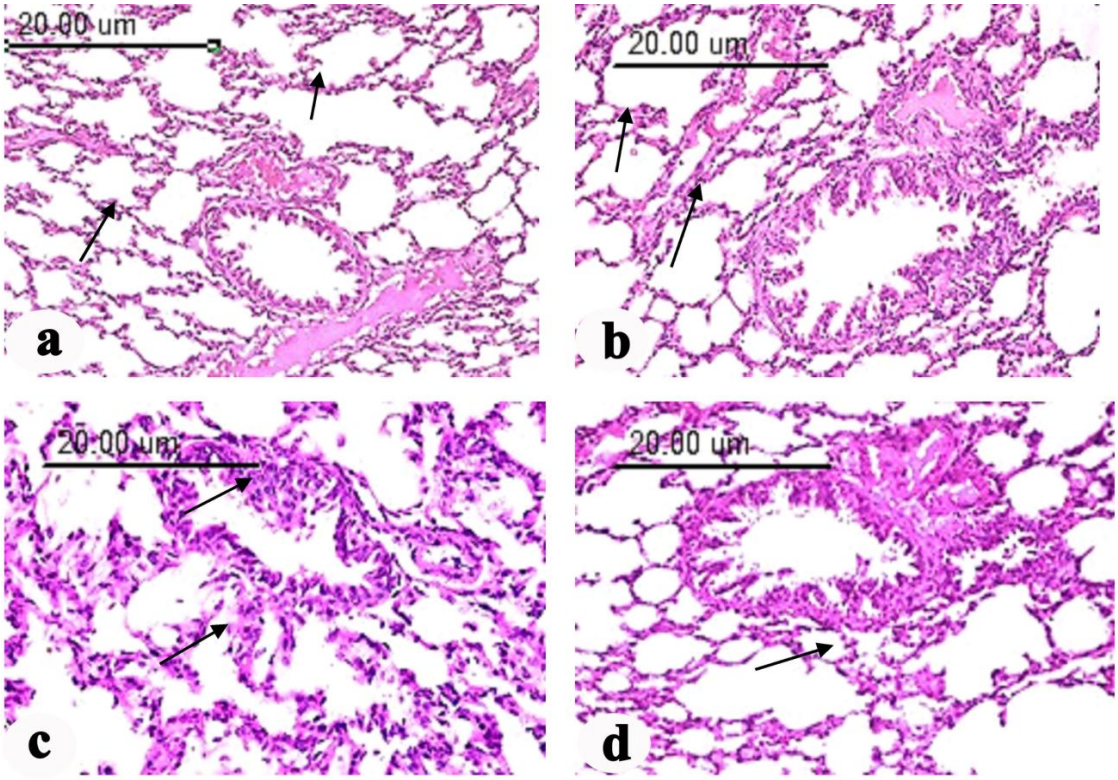

Fig. 4. Photomicrograph of lung tissue section: The groups designated as (a & b) control and ivermectin (3.7 mg/kg, taken orally for 14 days) exhibit typical lung architecture, with airspaces featuring delicate and fine inter-alveolar septa Arrow (c) of the 30 Gy irradiation group (5 fractions/week; in 10 fractions) demonstrates the metaplasia of the bronchiolar epithelial lining to stratified squamous cells and thickening of the inter-alveolar septa Arrow (d) illustrates the slight thickening of the alveolar interstitium arrow during concurrent therapy (Scale bar = 20µ).

Discussion

This study shows that in pulmonary tissues, IR increased the levels of PGE2, TGF-β1, FGF, and LDHA activity. Impaired lung function, oxidative stress, and inflammation are linked to IR induced pulmonary damage. These changes were associated with an increase in the TLR4/NF-κB/MAPK pathway and a histology indicator of lung injury. The current work demonstrated how ivermectin inhibits the TLR4/NF-κB/MAPK pathway to protect against IR induced oxidative stress and inflammatory damage.

As per earlier research (Rengachar et al., 2022; Jarzebska et al., 2021), lung tissues subjected to IR showed a large rise in MDA and NO levels, as well as a significant decrease in SOD activity and GSH content when compared to the control group.

By lowering the total cellular GSH levels, this results in significant abnormalities in oxidant/antioxidant status and glutathione-regulating enzymes which assist in the development of lung injury (Bledsoe et al., 2017).

Furthermore, NO promotes the synthesis of NF-κB and TGF-β1 (El kiki et al., 2021). Mitigation of oxidative stress would be expected to reduced lung damage. In this study, the combining administration of ivermectin with radiation greatly reduced the lung damage caused by radiation. When ivermectin and radiation were administered simultaneously, the pulmonary tissues demonstrate a significant rise in GSH content and SOD activity as well as a notable decrease in MDA and NO levels when compared to the irradiated group. The results suggest that ivermectin enhanced antioxidative capacities, which were essential for protecting against ROS-induced oxidative stress. The administration of ivermectin caused a significant increase in GST activity, indicating that this route is essential for the metabolism and elimination of ivermectin. The

reduction may be partially caused by the depletion of GSH activity (Domingues et al., 2016).

Lactate dehydrogenase (LDH) is the last enzyme in the metabolic pathway of anaerobic glycolysis, which converts glucose to lactate. According to Gupta (2022) Upregulation of LDH increases the death rate of individuals with cancer, viral infections such as SARS-CoV-2, and major inflammatory diseases.

Exposure to radiation increased TGF-β expression, which leads to the synthesis of lactate and LDHA, ultimately causing lung damage. Moreover, decreasing LDHA prevented radiation-induced extracellular matrix secretion by blocking TGF-β activation (Bancroft et al., 2013).

The results of the present investigation showed that ivermectin significantly decreased the radiation induced LDHA activity, suggesting that LDHA inhibition is a potential treatment target for radiation-induced lung damage. Ivermectin did not significantly harm intracellular respiratory activity, according to a previous study that demonstrated it induced a substantial repressing effect on the LDH activity of the cell line IB-RS-2, with no modifications in the activities of glucose-6-phosphate dehydrogenase and glucose-6-phosphatase (Mattei & Rodrigues, 1994). Arachidonic acid is the source of prostaglandins (PGs) lipid autacoids. Cyclooxygenase (COX) isoenzymes generate PGs lipid autacoids from arachidonate, and nonsteroidal anti-inflammatory drugs, like those that target COX-2 inhibition, work to stop them from forming (Ricciotti & FitzGerald,2011).

Consistent with the results of the present study, prior research has shown that radiation induces inflammation and increases the synthesis of pro-inflammatory PGE2 (Rengachar et al., 2022). The increased production of PGE2, which is observed in inflammatory conditions and following radiation exposure, may be an attempt to initiate the resolution of the inflammatory process once it reaches its peak. PGE2 has an anti-inflammatory impact *via* binding to the prostaglandin E receptor, which in turn modifies the actions of T lymphocytes and macrophages. These functions are crucial for both intrinsic and adaptive immunity as well as tissue restoration (Rengachar et al., 2022).

Triggered TLR4 complex may provide insight into the pathogenesis of numerous medical conditions, such as asthma, metabolic syndrome, autoimmune, neuroinflammatory, and cardiovascular disorders. Lung epithelial cells and immune cells both include TLRs. According to Yoshino et al. (2014) and Foy et al. (2019), concurrent with the current study, IR produces ROS, which in turn activates the TLR4 pathway, causes chronic inflammation, and initiates the activation of intracellular signaling pathways like NF-κB, which increases the production of ROS, RNS and pro-inflammatory cytokines. TLR4 activation and increased pro-inflammatory cytokine production, oxidative stress intensification, excessive ROS or RNS production, and collagen formation *via* myofibroblasts stimulated by ionizing radiation all influence TNF-α biological function.

In line with the current investigation, earlier research has demonstrated that the pathological process of radiation induced pulmonary damage is thought to include ROS-mediated DNA damage and the release of TGF-β1, TNF-α as well as FGF and NF-κB (Jin et al., 2020; Citrin et al., 2017; Vallée et al., 2017).

An increase in FGF-2 expression could be the result of a series of biological events in FGF-2-expressing cells responding to growth factors and cytokines such as TNF-α, TGF-β, and IL-1b brought on by radiation (Houchen et al., 1999). It is believed that radiation induces the free radical cascades, provoking the pro-inflammatory cytokines, TGF-α1 having a significant impact on the process of pulmonary toxicity (Rengachar et al., 2022).

Environmental stresses and a range of proinflammatory cytokines can initiate the MAPK p38 cascade. The MAPK pathway can be triggered by a variety of circumstances, including exposure to radiation, cytokines, growth hormones, toxins, and prescription drugs. Exposure to ionizing radiation has been established to either downregulate or activate a number of signaling pathways regulated by the MAPK superfamily. The MAPK p38 pathway was activated by oxidative stress (Rezatabar et al., 2019).

Radiation-induced pulmonary fibrosis is characterized by the accumulation of fibroblasts and myofibroblasts, which leads to considerable inflammatory cell infiltration, ECM remodeling, and finally fibrosis (Rengachar et al., 2022; Jin et al., 2020). Therefore, reducing IR induced myofibroblast differentiation is a crucial treatment strategy for avoiding fibrosis (Judge et al., 2017).

A previous study (Choi et al., 2015) found that injured epithelial cells induce a process called epithelial-mesenchymal transition (EMT), which initiates fibroblast manufacturing and activates the inflammatory cytokine responsible for fibrosis. The IR's stimulation of EMT is one of the processes that leads to lung fibrosis. The main cytokine in the EMT pathway is TGF-β. According to Jin et al. (2020), TGF-β initiates the process of epithelial cells transdifferentiating into activated myofibroblasts. The TGF-β signaling pathway obstructs the sequence of tissue fibrosis, which eventually results in the differentiation of pulmonary tissue and a loss of lung elasticity and function (Wei et al., 2019).

The findings of the present study demonstrated that concurrent administration of ivermectin and radiation therapy reduced the generation of inflammatory cytokines induced by radiation by impeding the NF-κB pathway's activation, blocking TLR4 signaling and MAPK activation, and reducing the release of prostaglandin E2 and NO (Zhang et al., 2008; Ci et al., 2009; Jiang et al., 2019). An effective strategy for treating inflammatory disorders may involve focusing on the TLR4 (ROS/RNS) radical series.

Conclusion

Ionizing radiation produces severe lung damage by increasing the production of cytokines, infiltration of alveolar macrophages, and creation of ROS. By reducing fibroblast differentiation and the generation of ROS and cytokines *via* the TLR4/NF-κB/MAPK pathway, Ivermectin protects against IR-induced lung injury.

Acknowledgments

Prof. Dr. Ahmed Osman (The Pathology Department, Faculty of Veterinary Medicine, Cairo University, Egypt) is greatly appreciated by the authors for his assistance in examining and documenting the histopathologic aspects of this work.

Conflict of interest

The authors declare no conflicts of interest

References

Azab, K. S., Meky, N. H., El-Deghidy, E. A. and Azoz, G. (2017) Response of COX2/PGE2 inflammatory pathway to brown seaweed extract in rats exposed to gamma radiation. *World Journal of Nuclear Science and Technology*, **7**(3), 189-205. DOI**:** 10.4236/wjnst.2017.73016

Bancroft, J.D., Stevens, A., Turner, D. R. (2013) Theory and Practice of Histological Techniques, 4th ed. Edinburgh, London, Melbourne, New York: Churchill Livingstone.

Bledsoe, T. J., Nath, S. K., and Decker, R. H. (2017) Radiation pneumonitis. *Clinics in chest medicine*, **38**(2), 201-208. DOI: 10.1016/j.ccm.2016.12.004

Buege, J. A. and Aust, S. D. (1978) Microsomal lipid peroxidation. In *Methods in enzymology* Vol. **52**, pp. 302-310. DOI: 10.1016/s0076-6879(78)52032-6

Caly, L., Druce, J. D., Catton, M. G., Jans, D. A. and Wagstaff, K. M. (2020). The FDA-approved drug ivermectin inhibits the replication of SARS-CoV-2 *in vitro*. *Antiviral Research*, **178**, 104787. DOI: 10.1016/j.antiviral.2020.104787

Choi, S. H., Hong, Z. Y., Nam, J. K., Lee, H. J., Jang, J., Yoo, R. J. and Lee, Y. J. (2015) A hypoxia-induced vascular endothelial-to-mesenchymal transition in development of radiation-induced pulmonary fibrosis. *Clinical Cancer Research*, **21**(16), 3716-3726. DOI: 10.1158/1078-0432.CCR-14-3193

Ci, X., Li, H., Yu, Q., Zhang, X., Yu, L., Chen, N., and Deng, X. (2009) Avermectin exerts anti-inflammatory effect by downregulating the nuclear transcription factor kappa-B and mitogen-activated protein kinase activation pathway. *Fundamental & Clinical Pharmacology*, **23**(4), 449-455. DOI: 10.1111/j.1472-8206.2009.00684.x

Citrin, D. E., Prasanna, P. G., Walker, A. J., Freeman, M. L., Eke, I., Barcellos-Hoff, M. H. and Coleman, C. N. (2017) Radiation-induced fibrosis: mechanisms and opportunities to mitigate. Report of an NCI workshop, September 19, 2016. *Radiation research*, **188**(1), 1-20. DOI: 10.1667/RR14784.1

Domingues, I., Oliveira, R., Soares, A.M. and Amorim M.J. (2016) Effects of ivermectin on Danio rerio: a multiple endpoint approach: behaviour, weight and subcellular markers. *Ecotoxicology.* **25**, 491-9 DOI: 10.1007/s10646-015-1607-5

El kiki, S. M., Mansour, H. H., Anis, L. M., Gabr, H. M. and Kamal, M. M. (2021) Evaluation of aromatase inhibitor on radiation induced pulmonary fibrosis *via* TGF-β/Smad 3 and TGF-β/PDGF pathways in rats. *Toxicology Mechanisms and Methods*, **31**(7), 538-545. DOI: 10.1080/15376516.2021.1934765

Eldh, T., Heinzelmann, F., Velalakan, A., Budach, W., Belka, C. and Jendrossek, V. (2012) Radiation-induced changes in breathing frequency and lung

histology of C57BL/6J mice are time-and dose-dependent. *Strahlentherapie und onkologie*, **188**(3), 274. DOI: 10.1007/s00066-011-0046-3

Elfakharany, Y. M., Elnagdy, S. A., Mohammad, N. S. and Morsy, M. M. (2021) Possible hepatotoxic effects in adult male albino rats on combination of ivermectin and paracetamol drugs used in CO-VID-19 infection management protocol. *Egyptian Society of Clinical Toxicology Journal*, **9**(2), 13-28. doi:10.21608/esctj.2021.105858.1004

Ellman, G.L. (1959) Tissue sulfhydryl groups. *Arch. Biochem. Biophys,* 17, 214-226. DOI: 10.1016/0003-9861(59)90090-6

Foy, B. D., Alout, H., Seaman, J. A., Rao, S., Magalhaes, T., Wade, M., ... & Dabiré, R. K. (2019). Efficacy and risk of harms of repeat ivermectin mass drug administrations for control of malaria (RIMDAMAL): a cluster-randomised trial. *The Lancet*, **393**(10180), 1517-1526. DOI: 10.1016/S0140-6736(18)32321-3

Gupta P.S., Biswal S., Panda S.K., Ray A.K. and Rana M. K. (2022) Binding mechanism and structural insights into the identified protein target of COVID-19 and importin-α with *in-vitro* effective drug ivermectin, *J Biomol Struct Dyn.* **40**: 2217-2226. DOI: 10.1080/07391102.2020.1839564

Gupta, G. S. (2022). The lactate and the lactate dehydrogenase in inflammatory diseases and major risk factors in COVID-19 patients. *Inflammation*, **45**(6), 2091-2123. DOI: 10.1007/s10753-022-01680-7

Houchen, C. W., George, R. J., Sturmoski, M. A. and Cohn, S. M. (1999) FGF-2 enhances intestinal stem cell survival and its expression is induced after radiation injury. *American Journal of Physiology-Gastrointestinal and Liver Physiology*, **276**(1), G249-G258. DOI: 10.1152/ajpgi.1999.276.1.G249

Ignarro, L. J., Buga, G. M., Wood, K. S., Byrns, R. E. and Chaudhuri, G. (1987) Endothelium-derived relaxing factor produced and released from artery and vein is nitric oxide. *Proceedings of the National Academy of Sciences*, **84**(24), 9265-9269. DOI: 10.1073/pnas.84.24.9265

Jarzebska, N., Karetnikova, E. S., Markov, A. G., Kasper, M., Rodionov, R. N. and Spieth, P. M. (2021) Scarred lung. An update on radiation-induced pulmonary fibrosis. *Frontiers in Medicine*, **7**, 1100. DOI: 10.3389/fmed.2020.585756

Jiang, L., Wang, P., Sun, Y. J. and Wu, Y. J. (2019) Ivermectin reverses the drug resistance in cancer cells through EGFR/ERK/Akt/NF-κB pathway. *Journal of Experimental & Clinical Cancer Research*, **38**(1), 1-18. DOI: 10.1186/s13046-019-1251-7

Jin, H., Yoo, Y., Kim, Y., Kim, Y., Cho, J. and Lee, Y. S. (2020) Radiation-induced lung fibrosis: preclinical animal models and therapeutic strategies. *Cancers*, **12**(6), 1561. DOI: 10.3390/cancers12061561

Judge, J. L., Lacy, S. H., Ku, W. Y., Owens, K. M., Hernady, E., Thatcher, T. H., ... and Kottmann, R. M. (2017) The lactate dehydrogenase inhibitor gossypol inhibits radiation-induced pulmonary fibrosis. *Radiation Research*, **188**(1), 35-43.

Kory, P., Meduri, G. U., Varon, J., Iglesias, J. and Marik, P. E. (2021) Review of the emerging evidence demonstrating the efficacy of ivermectin in the prophylaxis and treatment of COVID-19. *American journal of therapeutics*, **28**(3), e299 -e318. doi: 10.1097/MJT.0000000000001377..

Lotfy, D. M., Hasan, H. F. and Mostafa, D. M. (2022) Pulmonary prophylactic impact of bee venom against alterations induced by gamma irradiation *via* TLR4/NF-κB signaling pathway in rats. *Toxin Reviews*, **41**(4), 1199-1206.

Mattei, R. and Rodrigues, M. L. (1994) Effects of ivermectin on the activity of enzymes in mammalian cells *in vitro*. *Ecotoxicology and environmental safety*, **29**(3), 251-254. DOI: 10.1016/0147-6513(94)90001-9

Minami M. and Yoshikawa H. (1979) A simplified assay method of superoxide dismutase activity for clinical use. *Clin. Chim. Acta*., **92**: 337-342. DOI: 10.1016/0009-8981(79)90211-0

Mitsui, K., Ikedo, T., Kamio, Y., Furukawa, H., Lawton, M. T. and Hashimoto, T. (2020) TLR4 (Toll-Like Receptor 4) mediates the development of intracranial aneurysm rupture. *Hypertension*, **75**(2), 468-476.DOI: 10.1161/HYPERTENSIONAHA.118.12595

Rengachar, P., Bhatt, A. N., Polavarapu, S., Veeramani, S., Krishnan, A., Sadananda, M. and Das, U. N. (2022) Gamma-linolenic acid (GLA) protects against ionizing radiation-induced damage: An *In vitro* and *In vivo* study. *Biomolecules*, **12**(6), 797. DOI: 10.3390/biom12060797

Rezatabar S., Karimian A., Rameshknia V., Parsian H., Majidinia M., Kopi TA, Bishayee A, Sadeghinia A, Yousefi M, Monirialamdari M and Yousefi

B. (2019). RAS/MAPK signaling functions in oxidative stress, DNA damage response and cancer progression. *Journal of Cellular Physiology*.; **234**(9):14951-65. DOI: 10.1002/jcp.28334

Ricciotti E. and FitzGerald GA. (2011). Prostaglandins and inflammation. *Arteriosclerosis, Thrombosis, and Vascular Biology*. **31**: 986-1000. DOI: 10.1161/ATVBAHA.110.207449

Salami, S. and Karami-Tehrani, F. (2003). Biochemical studies of apoptosis induced by tamoxifen in estrogen receptor positive and negative breast cancer cell lines. *Clinical biochemistry*, **36**(4), 247-253. doi10.1016/S0009-9120(03)00007-9

Swargiary, A. (2020). Ivermectin as a promising RNA-dependent RNA polymerase inhibitor and a therapeutic drug against SARS-CoV2: *Evidence from in silico Studies*, 1-12. DOI:10.21203/rs.3.rs-73308/v1

Vallée, A., Lecarpentier, Y., Guillevin, R. and Vallée, J. N. (2017). Interactions between TGF-β1, canonical WNT/β-catenin pathway and PPAR γ in radiation-induced fibrosis. *Oncotarget*, **8**(52), 90579. DOI: 10.18632/oncotarget.21234

Wan, X., Shi, X., Li, M., Chen, Q., Xue, C., Li, G., ... and Liu, X. (2022). The Protective Effects and Mechanism of Doxepin on Radiation–Induced Lung Injury in Rats. *Dose-Response*, **20**(2), 15593258221107193. DOI: 10.1177/15593258221107193

Wei, P., Xie, Y., Abel, P. W., Huang, Y., Ma, Q., Li, L., ... and Tu, Y. (2019). Transforming growth factor (TGF)-β1-induced miR-133a inhibits myofibroblast differentiation and pulmonary fibrosis. *Cell Death & Disease*, **10**(9), 670. DOI: 10.1038/s41419-019-1873-x

Yan, S., Ci, X., Chen, N. A., Chen, C., Li, X., Chu, X., ... and Deng, X. (2011) Anti-inflammatory effects of ivermectin in mouse model of allergic asthma. *Inflammation Research*, **60**, 589-596 DOI: 10.1007/s00011-011-0307-8

Yang, S., Atkinson, S. C., Wang, C. *et al.,* (2020) The broad spectrum antiviral ivermectin targets the host nuclear transport importin α/β1 heterodimer. *Antiviral Research;* 177: 104760 DOI: 10.1016/j.antiviral.2020.104760

Yoshino, H., Chiba, K., Saitoh, T. and Kashiwakura, I. (2014) Ionizing radiation affects the expression of Toll-like receptors 2 and 4 in human monocytic cells through c-Jun N-terminal kinase activation. *Journal of Radiation Research*, **55**(5), 876-884. DOI: 10.1093/jrr/rru040

Zaidi, A. K. and Dehgani-Mobaraki, P. (2022) The mechanisms of action of ivermectin against SARS-CoV-2—an extensive review. *The Journal of Antibiotics*, **75**(2), 60-71. DOI: 10.1038/s41429-021-00491-6

Zhang, X., Song, Y., Ci, X., An, N., Ju, Y., Li, H., ... and Deng, X. (2008) Ivermectin inhibits LPS-induced production of inflammatory cytokines and improves LPS-induced survival in mice. *Inflammation Research*, **57**, 524-529. DOI: 10.1007/s00011-008-8007-8